ELSEVIER

Cement & Concrete Composites 25 (2003) 939–945

Cement & Concrete Composites

www.elsevier.com/locate/cemconcomp

The co-existence of thaumasite and ettringite in concrete exposed to magnesium sulfate at room temperature and the influence of blast-furnace slag substitution on sulfate resistance

P.W. Brown [a,*], R.D. Hooton [b], B.A. Clark [c]

[a] *Department of Materials Science and Engineering, Pennsylvania State University, 136 MRL, University Park, PA 16802, USA*
[b] *Department of Civil Engineering, University of Toronto, Toronto, Canada M5S 1A4*
[c] *RJ Lee Group, Monroeville, PA, USA*

Abstract

The effects of Type I Portland cement replacement by 45% or 72% blast-furnace slag on the sulfate resistance of laboratory concretes were analyzed by microstructural investigation. The concretes investigated were stored in water or in magnesium sulfate solutions for 23 years under laboratory conditions. For those stored in water only surface layers of carbonation and decalcification were observed. Concretes exposed to sulfate solutions formed brucite, ettringite and thaumasite. Thus, thaumasite was observed to form in concretes stored under laboratory conditions. In all cases both ettringite and thaumasite were found to co-exist in the damaged zones. However, the thaumasite appears to be moving in from the exterior after initial formation of ettringite, and has not resulted in the massive destruction of the hydrated matrix as has been found elsewhere at lower temperature exposures. Slag replacement was observed to be an effective means of conferring resistance to sulfate attack. Although the concretes studied were prepared at a W/cm (water-to-cementitious materials) ratio of 0.50, the depths of attack observed were comparable to those observed in concrete prepared at $w/c = 0.45$ using ASTM Type V (SRPC) cement alone.

Keywords: Ettringite; Slag; Sulfate resistance; Thaumasite; Brucite

1. Introduction

In a prior publication we described the effects of immersion of concrete produced using ASTM Type II (moderate sulfate-resisting) and Type V (highly sulfate-resisting) cements in sodium sulfate and magnesium sulfate solutions for approximately 20 years. That study explored the effects of the cement type, the water-to-cement ratio, and nature of the sulfate salt ($MgSO_4$ vs Na_2SO_4) on the sulfate resistance of the concrete. It was observed that ettringite and thaumasite had formed regardless of these parameters. Thaumasite formation under the test conditions was regarded as particularly significant in that the concretes were exposed to sulfate under laboratory conditions. The present work extends that study by evaluating the effect of blast-furnace slag on resistance to sulfate attack.

2. Experimental program

The concrete samples examined in this study were prepared in April 1977 as part of a study on the sulfate resistance of slag blended cement concretes. Based on a Bogue calculation, the ASTM Type I cement used contained 12.3% tricalcium aluminate (C_3A). The extent of slag replacement was 45% and 72% and the slag used contained: 39.7% CaO, 37.6% SiO_2, 8.5% Al_2O_3, 9.7% MgO, and 2.0% sulfide sulfur. Its Blaine fineness was 443 m^2/kg. The concretes were air-entrained and 20 mm crushed glacial gravel of mixed siliceous and carbonate content was used. Commercial ready mixed concretes supplied in 6 m^3 batches were used to prepare numerous concrete cylinders (75×150 mm). These were cast at room temperature. Molds were stripped after 48 h and the concretes were stored in water at 23 °C until compressive strengths of between 29.7 and 33.1 MPa were attained for the concretes studied in this paper. Subsequently, the cylinders were stored in 3000 ppm SO_4 (as $MgSO_4$) solution. Further details regarding cement

* Corresponding author. Tel.: +1-814-865-5352; fax: +1-814-863-7040/865-2-3260.
E-mail address: etx@psu.edu (P.W. Brown).

0958-9465/$ - see front matter © 2003 Published by Elsevier Ltd.
doi:10.1016/S0958-9465(03)00152-5

compositions and mix designs have been published elsewhere by Hooton and Emery [1]. Various concrete properties were monitored every 3 months for 4 years. The concretes were then stored in a laboratory warehouse (This warehouse was not temperature controlled but the building was heated during winter. The estimated temperature range is 23 ± 7 °C) until an age of 8 years when they were visually inspected. At that time it was decided to increase the sulfate exposure concentrations to accelerate the attack. All the exposed cylinders were immersed in 50,000 ppm SO_4 (as $MgSO_4$).Subsequent to this, they were again stored for 3 more years in the warehouse and then transferred to a 23 °C laboratory until they were retrieved for the present study at an age of 23 years.

The water-to-cementitious materials ratio (W/cm) was fixed at 0.50. Control concrete samples were produced at the same W/cm ratio and were immersed in water rather than in sulfate solution.

For this paper, samples were sliced from the cylinders using a diamond wheel saw in preparation for scanning electron microscope (SEM) analyses using back-scattered electron imaging. These were then epoxy impregnated, polished, and carbon coated. SEM combined with energy-dispersive X-ray (EDX) analyses were then carried out on the polished sections.

3. Results and discussion

The variable investigated in the present study is the effect of slag substitution (45% vs 72%) on the sulfate resistance of concrete. The water-to-cementitious materials ratio of all the samples studied was 0.50. Present results are compared to those of a previous study in which the sulfate resistance of concrete samples prepared using ASTM Type V sulfate-resistant cement containing 3.5% C_3A and ASTM Type II moderate-sulfate resistant cement containing 7.1% C_3A were studied [2].

3.1. Control samples immersed in water

Fig. 1 shows the near surface region of a concrete in which the cement paste has been substituted by 45% slag. As was observed for all the samples, a surface layer of calcium carbonate can be observed. In this specimen the layer is continuous and somewhat variable in thickness ranging between about 10 and 100 μm. Immediately behind the layer of calcium carbonate is a region of dark paste that has been decalcified as well as carbonated (see also Fig. 3). The effects of decalcification and carbonation were observed in both the EDX spectra and in the paste morphology. Fig. 2 shows unaltered paste only a few mm below the surface. The EDX spectra from these areas reveals an elevated Mg content compared to what would be expected in OPC paste. This is associated with the Mg content of the slag. Subsequent figures showing spectra from cement paste regions in concretes after having been exposed to magnesium sulfate will show higher Mg contents.

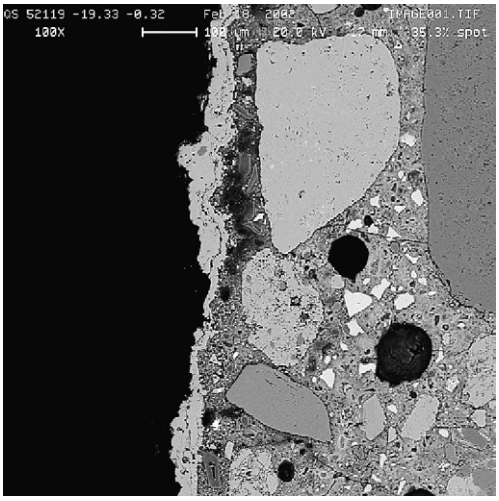

Fig. 1. Near-surface region.

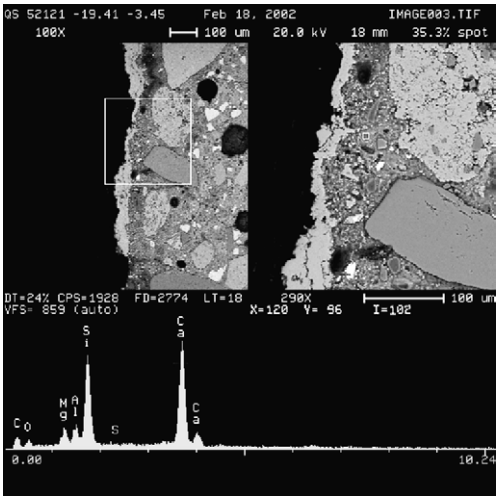

Fig. 2. Unaltered paste.

Fig. 3 shows the near-surface region of a concrete in which the cement paste has been substituted by 72% slag. A layer of carbonate is again present, likely due to dissolved CO_2 in the storage solutions for various parts of the 23-year exposure period. The EDX spectrum taken from a region immediately behind the carbonate layer at the location indicated shows this region to be decalcified in that the paste Ca/Si ratio is lower than would be expected for normal paste. Fig. 4 shows a region about 2 mm below the surface. The paste in this region shows a more normal Ca/Si ratio. In addition and in contrast to air voids filled with ettringite and/or thaumasite in concretes exposed to sulfate solutions,

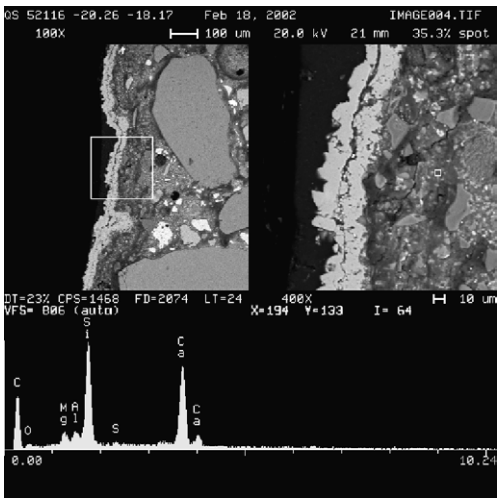

Fig. 3. Decalcified paste.

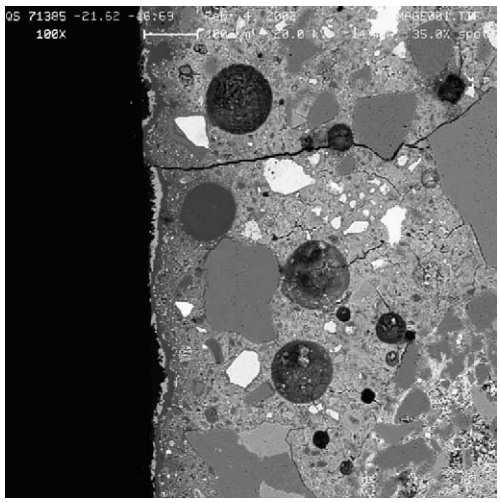

Fig. 5. Sulfate-exposed concrete.

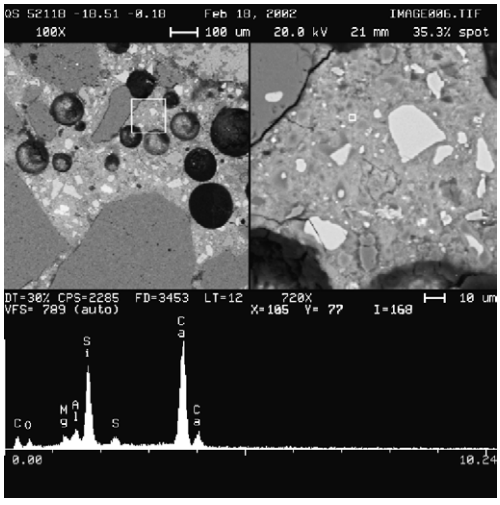

Fig. 4. Clean air voids.

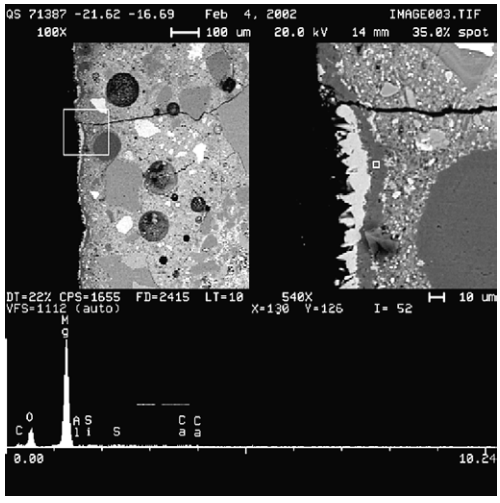

Fig. 6. Carbonated and brucite layers.

empty air voids can be observed for concrete which has only been cured in water.

3.2. Type I + 45% slag immersed in 50,000 ppm $MgSO_4$ solution

Fig. 5 shows the near-surface region. A surface deposit of $CaCO_3$ is observed as are filled air voids, cracks in the paste and a crack propagating inward through the paste and along the paste–aggregate interfaces. Fig. 6 illustrates that a structureless layer underlies the surface layer of calcium carbonate and the EDX spectrum of this layer indicates it to be brucite. Fig. 7 shows an air void filled with a structureless solid while the EDX spectrum confirms it to be brucite filled. An EDX spectrum of the paste in this region shows it to contain significant Mg while sulfate is also present, Fig. 8. Again, the paste morphology in this region is indicative

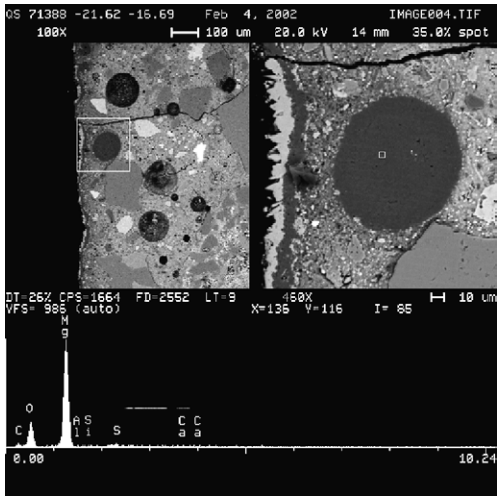

Fig. 7. Brucite-filled air void.

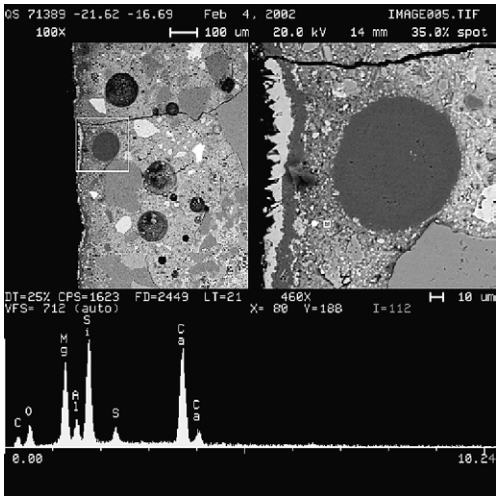

Fig. 8. Mg-enriched paste.

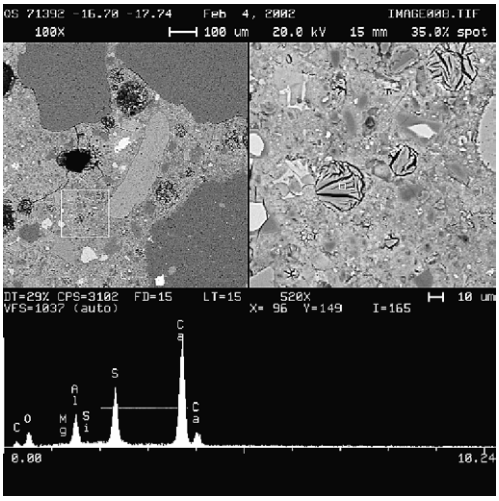

Fig. 10. Ettringite in air voids.

of carbonation. The grayscale gradient across the paste in this region illustrates the extent to which substantial Mg enrichment of the paste has occurred. This behavior is expected in the near-surface region as brucite deposits are recognized to block porosity and in doing so afford protection to the underlying paste.

Fig. 9 shows thaumasite filling an air void about 2 mm below the surface. While the fibrous microstructure of thaumasite cannot be discerned, the EDX spectrum is that of thaumasite. Cracks are present throughout the adjacent paste as had been previously observed by Crammond and Halliwell [6]. Unreacted slag particles surrounded by hydration rims can also be observed throughout the paste. Ettringite is distributed throughout the paste in this region and is likely responsible for the increased cracking observed.

The extent of cracking is reduced at a depth of about 4 mm below the surface, Fig. 10. Large air voids are only

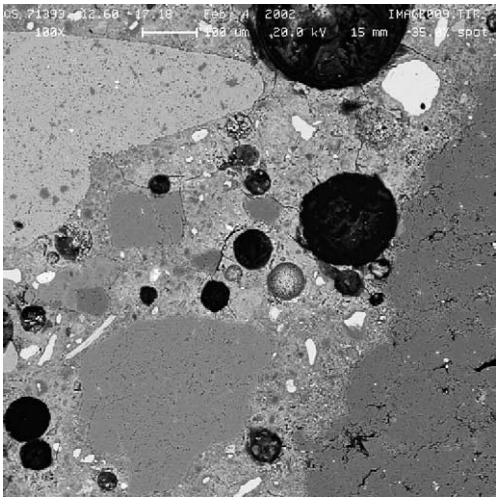

Fig. 11. Empty air voids.

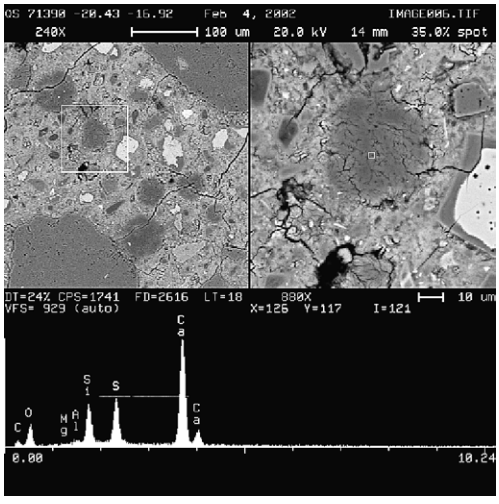

Fig. 9. Thaumasite-filled air void.

partially filled and the sulfate-containing phase present is ettringite, not thaumasite. Ettringite is observed to be filling the small air voids in a region where paste is not cracked and the EDX spectrum confirms ettringite. Fig. 11 at a depth of about 6 mm below the surface shows clean air voids.

3.3. Type I + 72% slag immersed in 50,000 ppm $MgSO_4$ solution

This sample showed surface and near surface features similar to those observed at 45% slag substitution. The extent of the region over which ettringite and thaumasite were observed was about 5 mm. Thus, slag substitution over the compositional range examined has the beneficial effect of limiting sulfate attack to a depth of a few millimeters.

Analysis of the materials filling air voids in this region indicates assemblages comprised of ettringite, thaumasite, and calcium silicate hydrate. Fig. 12 shows such a filled air void that is surrounded by slag particles. The spectrum in Fig. 12 suggests the presence of both ettringite and thaumasite. The spectrum taken at a different location at the periphery of this air void shows calcium silicate hydrate, Fig. 13. The composite nature of the filled air voids is strikingly shown in Fig. 14 where four morphologically distinct solids are apparent. Fig. 15 shows a second composite filled air void. The spectrum in the region shown is that of thaumasite. The phase assemblage contributing to the spectrum of the region shown in Fig. 16 is indeterminate but may be either decalcified C–S–H or a mixture of calcium carbonate and hydrous silica. Fig. 17 shows a spectrum of calcium carbonate, suggesting the assemblage in Fig. 16 to be calcium carbonate and silica. Accepting this

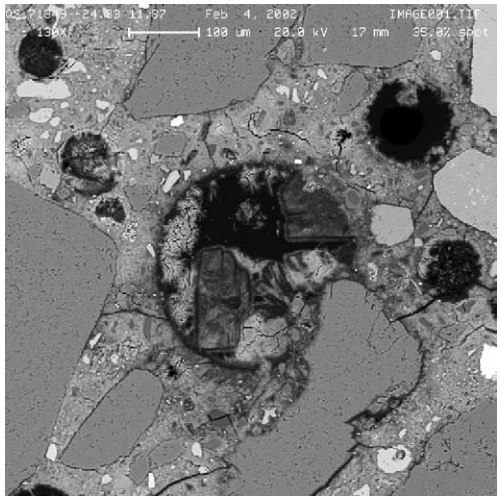

Fig. 14. Multiple solids in an air void.

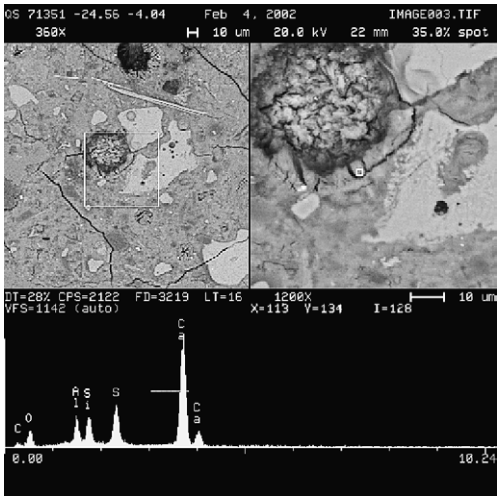

Fig. 12. Ettringite and thaumasite filling an air void.

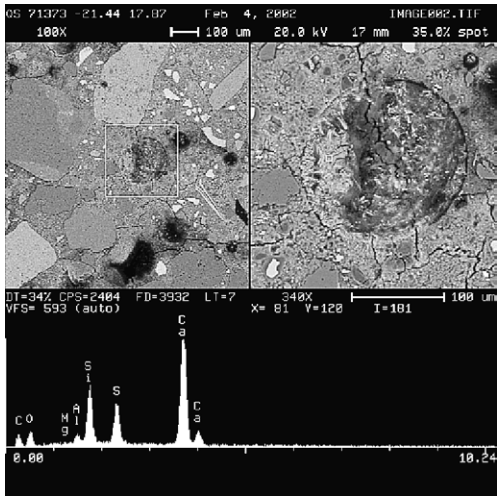

Fig. 15. Thaumasite in an air void.

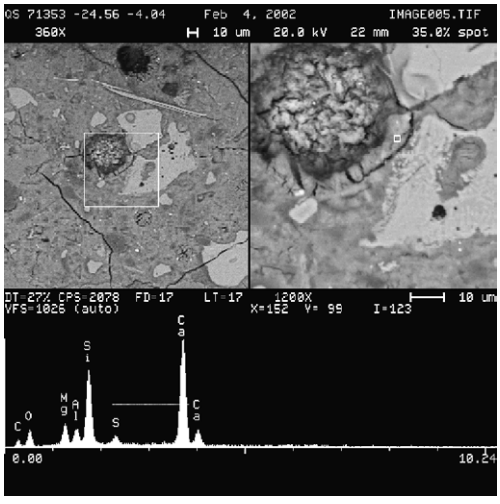

Fig. 13. C–S–H.

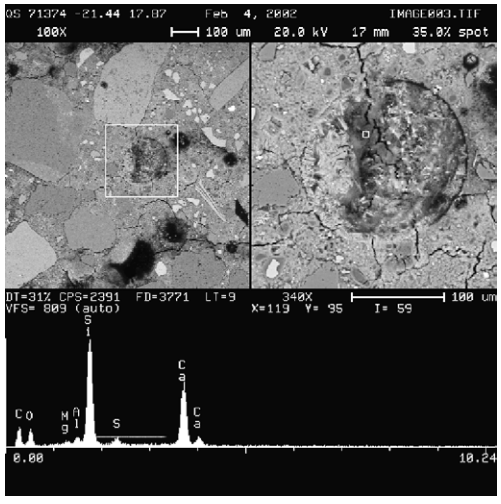

Fig. 16. Undetermined phase in void.

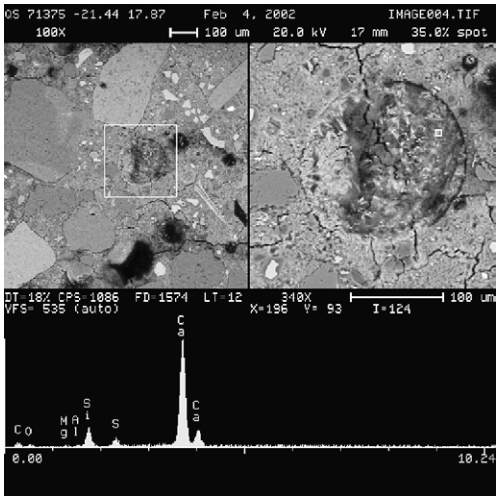

Fig. 17. Calcium carbonate in air void.

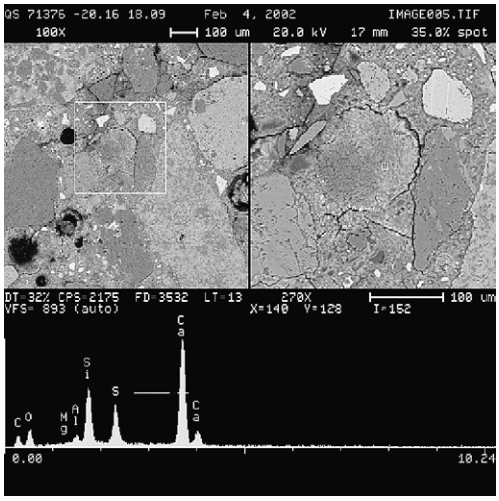

Fig. 18. Thaumasite-filled air void.

assumption, suggests the mechanism of thaumasite formation that involves the progression of a carbonate front that decomposes the C–S–H to $CaCO_3$ and $SiO_2 \cdot nH_2O$ followed by the ingress of sulfate to permit thaumasite formation. Fig. 18 shows an air void entirely filled with thaumasite indicating the mechanistic steps suggested have gone to completion.

4. Conclusions

Both ettringite and thaumasite were observed to form in the near-surface zone of the slag blended cement concretes studied. Until recently, thaumasite formation was regarded to be favorable only at relatively low temperatures. The present study along with prior work [2,3,5] indicates it will form at room temperature regardless of whether the cement used is ASTM Type V, Type II or a Type I-slag blend.

Table 1
Depth of sulfate attack after long-term exposure

Cement type	w/c ratio	Attacking species	Duration of exposure (years)	Depth of attack (mm)
V	0.45	$MgSO_4$	21	7
II	0.50	$MgSO_4$	21	32
I + 45% slag	0.50	$MgSO_4$	23	6
I + 72% slag	0.50	$MgSO_4$	23	5

As in prior studies [3,5], the depth to which thaumasite was observed was less than that for ettringite. This likely resulted from subsequent carbonate ingress into the ettringite damaged surface layer. The formation of and distributions of ettringite and thaumasite, along with brucite, are similar to those observed in sulfate-resisting cement concretes previously analyzed [3,5]. However, the extent of sulfate attack showed a major dependence on slag substitution. Table 1 compares the depth of attack depending on the cement type and the w/c ratio:

As can be seen, slag substitutions for the range investigated are highly effective in conferring improved sulfate resistance to concrete. Such a finding is consistent with work showing permeability reductions associated with slag substitutions [4]. It seems significant that the substitution of Type I cement by slag results in sulfate resistance comparable to that of a concrete containing Type V cement, even when the latter is produced at a lower w/c ratio. Further, slag substitution improved sulfate resistance even though the aluminate content of the Type I cement in these concretes was substantially higher than that in the previously studied concretes made using Type II or Type V cements. These observations reconfirm the well-accepted view that permeability reduction is more important in achieving sulfate resistance than is compositional control.

Acknowledgements

The authors would like to acknowledge John Emery of John Emery Geotechnical Engineering Ltd. for initiating the original program and for having the foresight to keep the concrete specimens in sulfate exposure.

References

[1] Hooton RD, Emery JJ. Sulfate resistance of a canadian slag cement. ACI Mater J 1990;87(6):547–55.
[2] Brown PW, Hooton RD. Ettringite and thaumasite formation in laboratory concretes prepared using sulfate-resisting cements. Cem Concr Compos, in press.

[3] Brown PW, Doerr A. Chemical changes in concrete due to the ingress of aggressive species. Cem Concr Res 2000;31:411–8.
[4] McGrath PF, Hooton RD. Influence of binder composition on chloride penetration of concrete. Durab Concr 1997;ACI SP-170:331–47.
[5] Hooton RD, Brown PW. Microscopic examination of sulphate-resistant concretes exposed to sulphate solutions for 21 years. 8th Euroseminar on Microscopy Applied to Building Materials. 2001. p. 147–57.
[6] Crammond NJ, Halliwell MA. The thaumasite form of sulfate attack in concretes containing a source of carbonate ions. In: Malhotra VM, editor. 2nd Symposium On Advances in Concrete Technology, ACI SP154. 1995. p. 357–80.